

Fuzzy Logic Controller Based APF with Advanced Power Quality

SAMAR GAMARE¹, ADVAY DONGRE²

¹B.Tech, Dept of EE, Veermata Jijabai Institute of Technology College, Mumbai ,Matunga, Maharashtra, India.

² B.Tech, Dept of EE, Veermata Jijabai Institute of Technology College, Mumbai ,Matunga, Maharashtra, India.

Abstract: Design of a fuzzy logic controller by using voltage as feedback for significantly improving the dynamic performance of proposed APF module. Utility distribution networks, sensitive industrial loads and critical commercial operations suffer from various types of outages and service interruptions which can cost significant financial losses. An active power filter implemented with a four-leg voltage-source inverter using a predictive control scheme is presented. The use of a four-leg voltage-source inverter allows the compensation of current harmonic components, as well as unbalanced current generated by single-phase nonlinear loads. A detailed yet simple mathematical model of the active power filter, including the effect of the equivalent power system impedance, is derived and used to design the predictive control algorithm. The compensation performance of the proposed active power filter and the associated intelligence control scheme under steady state and transient operating conditions is demonstrated to improve the power quality is simulated using MATLAB/SIMULINK.

Keywords: Fuzzy Logic Controller, Active Power Filter, Current Control, Four-Leg Converters, Predictive Controlharmonics, and Power Quality.

I. INTRODUCTION

Increasing global energy consumption and noticeable environmental pollution are making renewable energy more important. Today, a small percentage of total global energy comes from renewable sources, mainly hydro and wind power. As more countries try to reduce greenhouse gas (GHG) emissions, new power generation capacity can no longer be met by traditional methods such as burning coal, oil, natural gas, etc. However, these DG units produce a wide range of voltages [1] due to the fluctuation of energy resources and impose stringent requirements for the inverter topologies and controls. To have sustainable growth and social progress, it is necessary to meet the energy need by utilizing the renewable energy resources like wind, biomass, hydro, co-generation, etc. In sustainable energy system, energy conservation and the use of renewable source are the key paradigm. The need to integrate the renewable energy like wind energy/PV into power system is to make it possible to minimize the environmental impact on conventional plant [1]. The integration of wind energy into existing power system presents technical challenges and that requires consideration of voltage regulation, stability, power quality problems. The power quality is an essential customer-focused measure and is greatly affected by the operation of a distribution and transmission network. The issue of power quality is of great importance to the wind turbine [2]. There has been an extensive growth and quick development in the exploitation of wind energy in recent years. Although active power filters implemented with three-phase four-leg voltage-source inverters (4L-VSI) have already been presented in the technical literature [2]–[6], the primary contribution of this

paper is a predictive control algorithm designed and implemented specifically for this application.

Traditionally, active power filters have been controlled using pre-tuned controllers, such as PI-type or adaptive, for the current as well as for the dc-voltage loops [7], [8]. PI controllers must be designed based on the equivalent linear model, while predictive controllers use the nonlinear model, which is closer to real operating conditions. An accurate model obtained using predictive controllers improves the performance of the active power filter, especially during transient operating conditions, because it can quickly follow the current-reference signal while maintaining a constant dc-voltage. So far, implementations of predictive control in power converters have been used mainly in induction motor drives [9]–[16]. Conventionally, PI, PD and PID controller are most popular controllers and widely used in most power electronic appliances however recently there are many researchers reported successfully adopted Fuzzy Logic Controller (FLC) to become one of intelligent controllers to their appliances [3]. With respect to their successful methodology implementation, this kind of methodology implemented in this paper is using fuzzy logic controller with feed back by introduction of voltage respectively. The introduction of change in voltage in the circuit will be fed to fuzzy controller to give appropriate measure on steady state signal. The fuzzy logic controller serves as intelligent controller for this propose. This paper presents the mathematical model of the 4L-VSI and the principles of operation of the proposed predictive control scheme, including the design procedure. The complete description of

the selected current reference generator implemented in the active power filter is also presented. Finally, the proposed active power filter and the effectiveness of the associated control scheme compensation, power quality improvement is simulated using MATLAB/SIMULINK.

II. FOUR-LEG CONVERTER MODEL

It consists of various types of power generation units and different types of loads. Renewable sources, such as wind and sunlight, are typically used to generate electricity for residential users and small industries. Both types of power generation use ac/ac and dc/ac static PWM converters for voltage conversion and battery banks for long term energy storage. These converters perform maximum power point tracking to extract the maximum energy possible from wind and sun. The electrical energy consumption behavior is random and unpredictable, and therefore, it may be single- or three-phase, balanced or unbalanced, and linear or nonlinear. An active power filter is connected in parallel at the point of common coupling to compensate current harmonics, current unbalance, and reactive power. It is composed by an electrolytic capacitor, a four-leg PWM converter, and a first-order output ripple filter, as shown in Fig. 1. This circuit considers the power system equivalent impedance Z_s , the converter output ripple filter impedance Z_f , and the load impedance Z_L . The four-leg PWM converter topology is shown in Fig. 2. This converter topology is similar to the conventional three-phase converter with the fourth leg connected to the neutral bus of the system. The fourth leg increases switching states from improving control flexibility and output voltage quality [19], and is suitable for current unbalanced compensation.

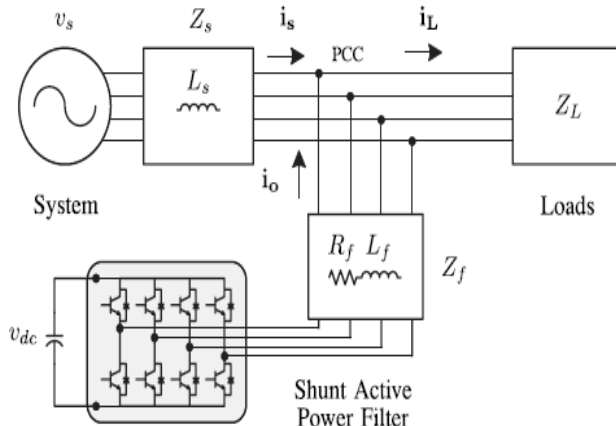


Fig. 1. Three-phase equivalent circuit of the proposed shunt active power filter.

The voltage in any leg x of the converter, measured from the neutral point (n), can be expressed in terms of switching states, as follows:

$$v_{xn} = S_x - S_n v_{dc}, \quad x = u, v, w, n. \quad (1)$$

The mathematical model of the filter derived from the equivalent circuit shown in Fig. 1 is

$$\mathbf{v}_o = v_{xn} - R_{eq} \mathbf{i}_o - L_{eq} \frac{d \mathbf{i}_o}{dt} \quad (2)$$

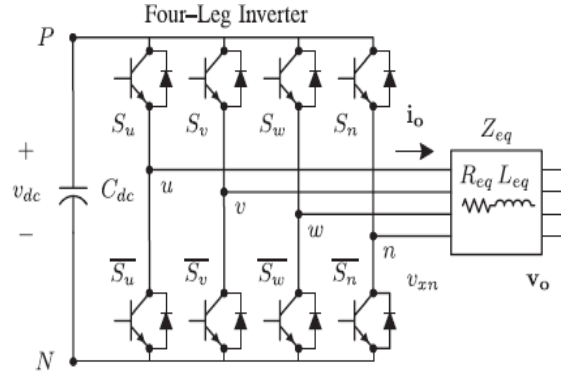


Fig.2. Two-level four-leg PWM-VSI topology.

Where R_{eq} and L_{eq} are the 4L-VSI output parameters expressed as Thevenin's impedances at the converter output terminals Z_{eq} . Therefore, the Thevenin's equivalent impedance is determined by a series connection of the ripple filter impedance Z_f and a parallel arrangement between the system equivalent impedance Z_s and the load impedance Z_L .

$$Z_{eq} = \frac{Z_s Z_L}{Z_s + Z_L} + Z_f \approx Z_s + Z_f \quad (3)$$

For this model, it is assumed that $Z_L \gg Z_s$, that the resistive part of the system's equivalent impedance is neglected, and that the series reactance is in the range of 3–7% p.u., which is an acceptable approximation of the real system. Finally,

$$R_{eq} = R_f \text{ and } L_{eq} = L_s + L_f \quad (4)$$

III. REFERENCE CURRENT GENERATION SCHEME

A dq-based current reference generator scheme is used to obtain the active power filter current reference signals. This scheme presents a fast and accurate signal tracking capability. This characteristic avoids voltage fluctuations that deteriorate the current reference signal affecting compensation performance [20]. The current reference signals are obtained from the corresponding load currents as shown in Fig. 3. This module calculates the reference signal currents required by the converter to compensate reactive power, current harmonic and current imbalance. The displacement power factor ($\sin \phi(L)$) and the maximum total harmonic distortion of the load ($THD(L)$) defines the relationships between the apparent power required by the active power filter, with respect to the load, as shown

$$\frac{S_{APF}}{S_L} = \frac{\sqrt{\sin \phi(L) + THD(L)^2}}{\sqrt{1 + THD(L)^2}} \quad (5)$$

Where the value of $THD(L)$ includes the maximum compensable harmonic current, defined as double the sampling frequency f_s . The frequency of the maximum current harmonic component that can be compensated is equal to one half of the converter switching frequency. The dq-based scheme operates in a rotating reference frame; therefore, the measured currents must be multiplied by the $\sin(\omega t)$ and $\cos(\omega t)$ signals. By using dq-transformation, the d current component is synchronized with the corresponding phase-to-neutral system voltage, and the q current component

is phase-shifted by 90°. The $\sin(\omega t)$ and $\cos(\omega t)$ synchronized reference signals are obtained from a synchronous reference frame (SRF) PLL [21]. The SRF-PLL generates a pure sinusoidal waveform even when the system voltage is severely distorted. Tracking errors are eliminated, since SRF-PLLs are designed to avoid phase voltage unbalancing, harmonics (i.e., less than 5% and 3% in fifth and seventh, respectively), and offset caused by the nonlinear load conditions and measurement errors [3], the relationship between the real currents $i_{Lx}(t)$ ($x = u, v, w$) and the associated dq components (i_d and i_q).

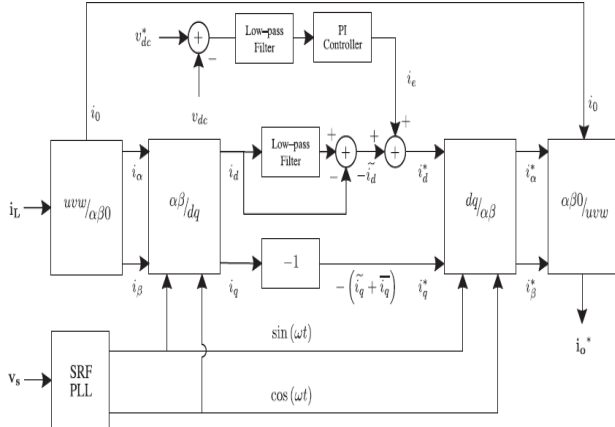


Fig. 3. dq-based current reference generator block diagram.

$$\begin{bmatrix} i_d \\ i_q \end{bmatrix} = \sqrt{\frac{2}{3}} \begin{bmatrix} \sin \omega t & \cos \omega t \\ -\cos \omega t & \sin \omega t \end{bmatrix} \begin{bmatrix} 1 & -\frac{1}{2} & -\frac{1}{2} \\ 0 & \frac{\sqrt{3}}{2} & -\frac{\sqrt{3}}{2} \end{bmatrix} \begin{bmatrix} i_{Lu} \\ i_{Lv} \\ i_{Lw} \end{bmatrix} \quad (6)$$

A low-pass filter (LPF) extracts the dc component of the phase currents i_d to generate the harmonic reference components i_d^* . The reactive reference components of the phase-currents are obtained by phase-shifting the corresponding ac and dc components of i_q by 180°. In order to keep the dc-voltage constant, the amplitude of the converter reference current must be modified by adding an active power reference signal i_e with the d-component. The resulting signals i_d^* and i_q^* are transformed back to a three-phase system by applying the inverse Park and Clark transformation. The cut off frequency of the LPF used in this paper is 20 Hz.

$$\begin{bmatrix} i_{ou}^* \\ i_{ov}^* \\ i_{ow}^* \end{bmatrix} = \sqrt{\frac{2}{3}} \begin{bmatrix} \frac{1}{\sqrt{2}} & 1 & 0 \\ \frac{1}{\sqrt{2}} & -\frac{1}{2} & \frac{\sqrt{3}}{2} \\ \frac{1}{\sqrt{2}} & -\frac{1}{2} & -\frac{\sqrt{3}}{2} \end{bmatrix} \times \begin{bmatrix} 1 & 0 & 0 \\ 0 & \sin \omega t & -\cos \omega t \\ 0 & \cos \omega t & \sin \omega t \end{bmatrix} \begin{bmatrix} i_0 \\ i_d^* \\ i_q^* \end{bmatrix} \quad (7)$$

The current that flows through the neutral of the load is compensated by injecting the same instantaneous value obtained from the phase-currents, phase-shifted by 180°, as shown next.

$$i_{on}^* = -(i_{Lu} + i_{Lv} + i_{Lw}) \quad (8)$$

One of the major advantages of the dq-based current reference generator scheme is that it allows the implementation of a linear controller in the dc-voltage control loop. However, one important disadvantage of the dq-based current reference frame algorithm used to generate the current reference is that a second order harmonic component is generated in i_d and i_q under unbalanced operating conditions. The amplitude of this harmonic depends on the percent of unbalanced load current (expressed as the relationship between the negative sequence current $i_{L,2}$ and the positive sequence current $i_{L,1}$). The second-order harmonic cannot be removed from i_d and i_q , and therefore generates a third harmonic in the reference current when it is converted back to abc frame [17]. Since the load current does not have a third harmonic, the one generated by the active power filter flows to the power system.

A. DC Link Voltage Control

The dc-voltage converter is controlled with a traditional PI controller. This is an important issue in the evaluation, since the cost function is designed using only current references, in order to avoid the use of weighting factors. Generally, these weighting factors are obtained experimentally, and they are not well defined when different operating conditions are required. Additionally, the slow dynamic response of the voltage across the electrolytic capacitor does not affect the current transient response. For this reason, the PI controller represents a simple and effective alternative for the dc-voltage control. The dc-voltage remains constant (with a minimum value of sqrt of 6vs(rms)) until the active power absorbed by the converter decreases to a level where it is unable to compensate for its losses. The active power absorbed by the converter is controlled by adjusting the amplitude of the active power reference signal i_e , which is in phase with each phase voltage. In the block diagram shown in Fig. 4, the dc-voltage v_{dc} is measured and then compared with a constant reference value v_{dc}^* . The error (e) is processed by a PI controller, with two gains, K_p and T_i . Both gains are calculated according to the dynamic response requirement. Fig. 4 shows that the output of the PI controller is fed to the dc-voltage transfer function $G(s)$ which is represented by a first-order system.

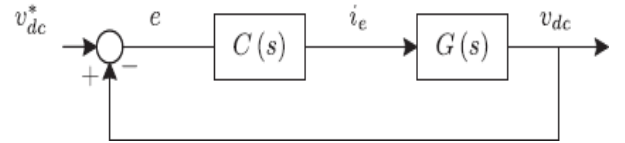


Fig. 4. DC-voltage control block diagram.

$$G(s) = \frac{v_{dc}}{i_e} = \frac{3}{2} \frac{K_p v_s \sqrt{2}}{C_{dc} v_{dc}^*} \quad (9)$$

The equivalent closed-loop transfer function of the given system with a PI controller

$$C(s) = K_p \left(1 + \frac{1}{T_i \cdot s} \right)$$

$$\frac{v_{dc}}{i_e} = \frac{\frac{\omega_n^2}{a} \cdot (s + a)}{s^2 + 2\zeta\omega_n \cdot s + \omega_n^2} \quad (10)$$

Since the time response of the dc-voltage control loop does not need to be fast, a damping factor $\zeta = 1$ and a natural angular speed $\omega_n = 2\pi \cdot 100$ rad/s are used to obtain a critically damped response with minimal voltage oscillation. The corresponding integral time $T_i = 1/a$ (13) and proportional gain K_p can be calculated as

$$\zeta = \sqrt{\frac{3}{8} \frac{K_p v_s \sqrt{2 T_i}}{C_{dc} v_{dc}^*}}$$

$$\omega_n = \sqrt{\frac{3}{2} \frac{K_p v_s \sqrt{2}}{C_{dc} v_{dc}^* T_i}}. \quad (11)$$

IV. INTRODUCTION TO FUZZY LOGIC CONTROLE

L. A. Zadeh presented the first paper on fuzzy set theory in 1965. Since then, a new language was developed to describe the fuzzy properties of reality, which are very difficult and sometime even impossible to be described using conventional methods. Fuzzy set theory has been widely used in the control area with some application to power system [5]. A simple fuzzy logic control is built up by a group of rules based on the human knowledge of system behavior. Matlab/Simulink simulation model is built to study the dynamic behavior of converter. Furthermore, design of fuzzy logic controller can provide desirable both small signal and large signal dynamic performance at same time, which is not possible with linear control technique. Thus, fuzzy logic controller has been potential ability to improve the robustness of converters. The basic scheme of a fuzzy logic controller is shown in Fig 5 and consists of four principal components such as: a fuzzification interface, which converts input data into suitable linguistic values; a knowledge base, which consists of a data base with the necessary linguistic definitions and the control rule set; a decision-making logic which, simulating a human decision process, infer the fuzzy control action from the knowledge of the control rules and linguistic variable definitions; a de-fuzzification interface which yields non fuzzy control action from an inferred fuzzy control action [10] as shown in Fig.6.

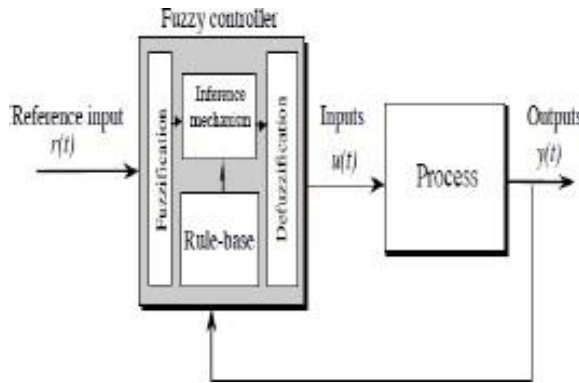


Fig.5. General Structure of the fuzzy logic controller.

The fuzzy control systems are based on expert knowledge that converts the human linguistic concepts into an automatic control strategy without any complicated mathematical model [10]. With the hysteresis control, limit bands are set on either side of a signal representing the desired output waveform [6] as shown in Fig.7. The inverter switches are

operated as the generated signals within limits. The control circuit generates the sine reference signal wave of desired magnitude and frequency, and it is compared with the actual signal. As the signal exceeds a prescribed hysteresis band, the upper switch in the half bridge is turned OFF and the lower switch is turned ON. As the signal crosses the lower limit, the lower switch is turned OFF and the upper switch is turned ON. The actual signal wave is thus forced to track the sine reference wave within the hysteresis band limits.

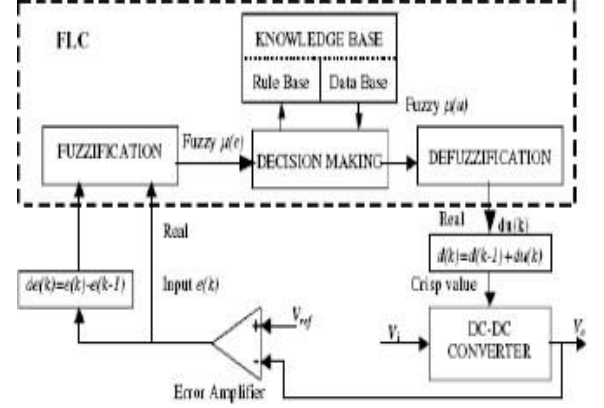


Fig.6. Block diagram of the Fuzzy Logic Controller (FLC) for proposed converter.

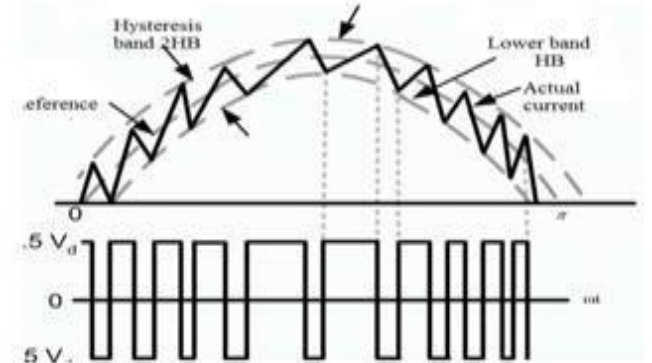


Fig.7. Hysteresis current Modulation.

VI. MATLAB MODELEING AND SIMULATION RESULTS

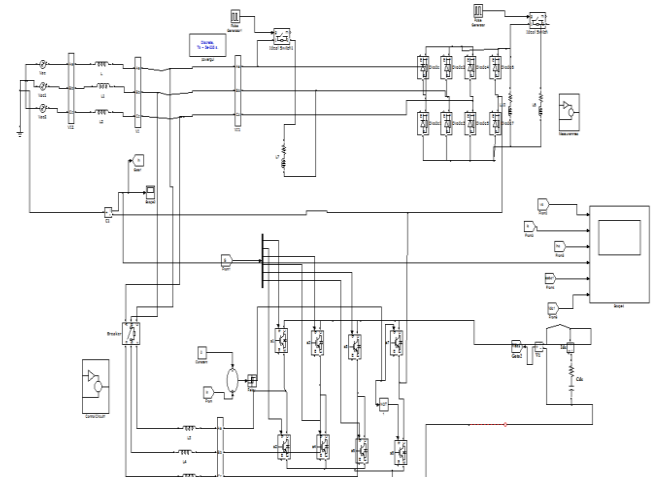


Fig.8 Matlab/Simulink Model of Proposed RES Fed 4-Leg APF system with formal PI & Intelligence Controllers.

Fig.8. Matlab/Simulink Model of Proposed RES Fed 4-Leg APF system with formal PI & Intelligence Controllers.

Case1: Proposed RES Fed APF with Conventional PI Controller

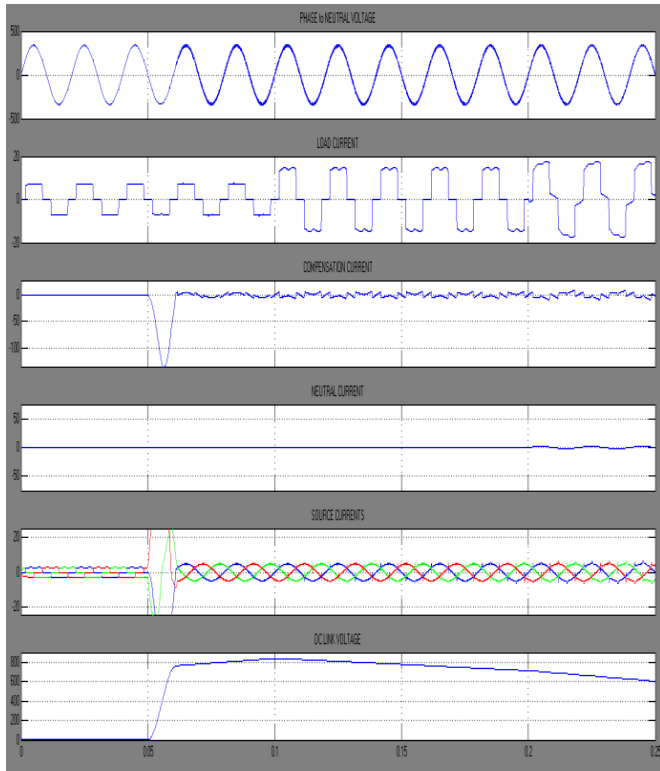


Fig.9. Simulation results for APF with Formal PI Controller (a) Source Voltage. (b) Load current. (c) Compensator Current. (d) Neutral Current, (e) Source Current (f) DC Link Voltage.

Fig.9. Simulation results for APF with Formal PI Controller (a) Source Voltage. (b) Load current. (c) Compensator Current, (d) Neutral Current, (e) Source Current (f) DC Link Voltage. Here compensator is turned on at 0.05 seconds, before we get some harmonics coming from non-linear load, then distorts our parameters and get sinusoidal when compensator is in on.

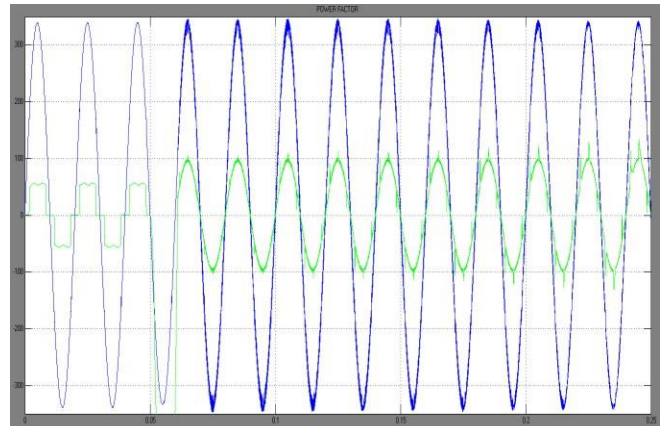


Fig.10 Power Factor for APF with Conventional PI Controller.

Fig. 10 shows the power factor it is clear from the figure after compensation power factor is unity.

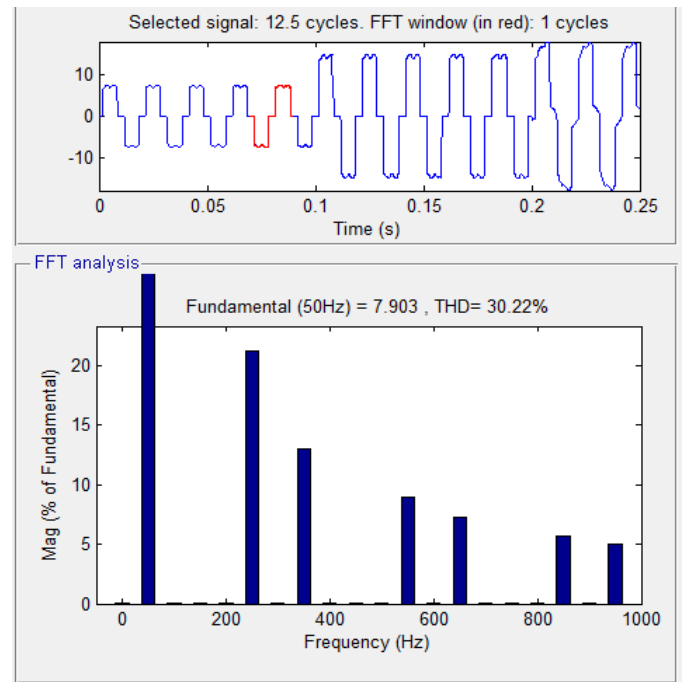


Fig. 11. FFT Analysis of Phase-A Source Current for without compensation scheme.

Fig.11 shows the FFT Analysis of Phase-A Source Current without any compensation, here we get 30.22%.

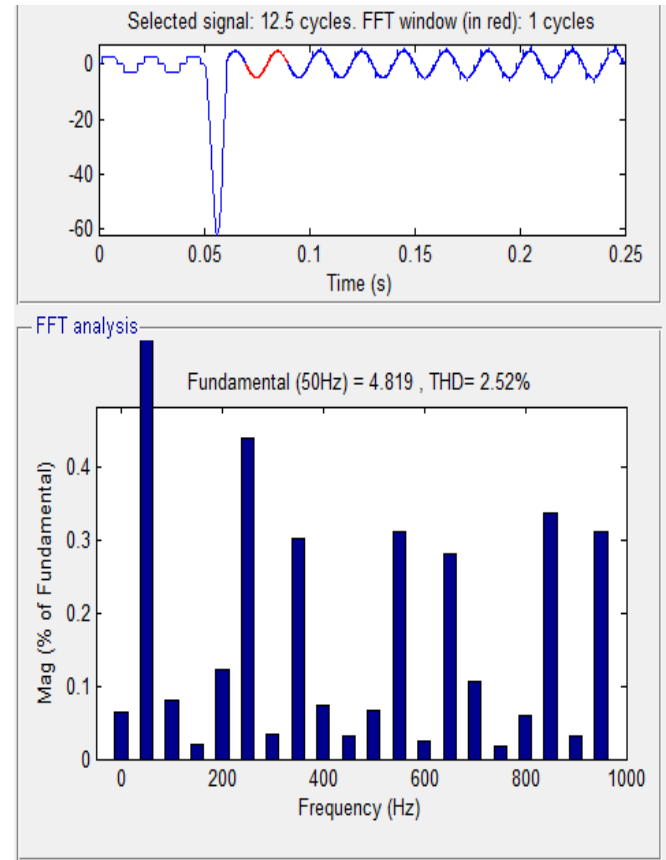


Fig. 12. FFT Analysis of Phase-A Source Current with PI Controlled APF.

Fig.12 shows the FFT Analysis of Phase-A Source Current with PI Controlled APF, here we get 2.52%.

Case 2: Proposed APF with Intelligence based Fuzzy Controller

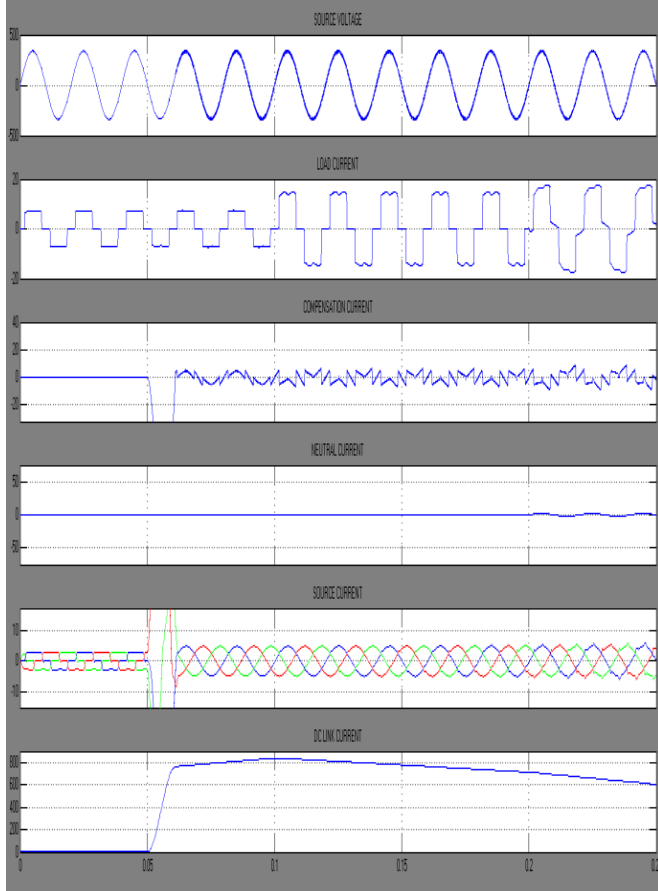


Fig.13 Simulation results for APF with Fuzzy Controller
 (a) Source Voltage. (b) Load current. (c) Compensator Current. (d) Neutral Current, (e) Source Current (f) DC Link Voltage.

Fig.13 Simulation results for APF with Fuzzy Controller
 (a) Source Voltage. (b) Load current. (c) Compensator Current, (d) Neutral Current, (e) Source Current (f) DC Link Voltage. Here compensator is turned on at 0.05 seconds, before we get some harmonics coming from non-linear load, then distorts our parameters and get sinusoidal when compensator is in on.

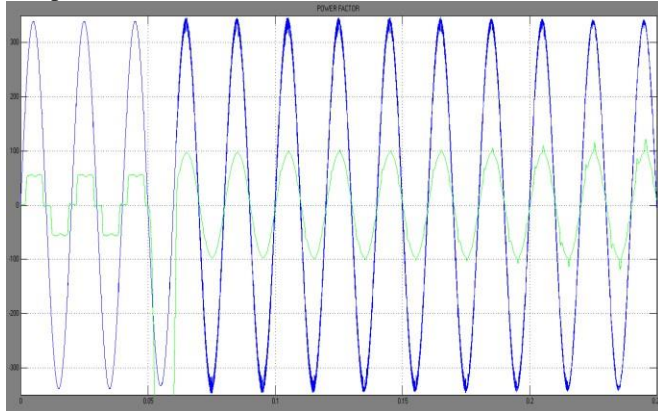


Fig.14 Power Factor for APF with Fuzzy Controller.

Fig. 14 shows the power factor it is clear from the figure after compensation power factor is unity.

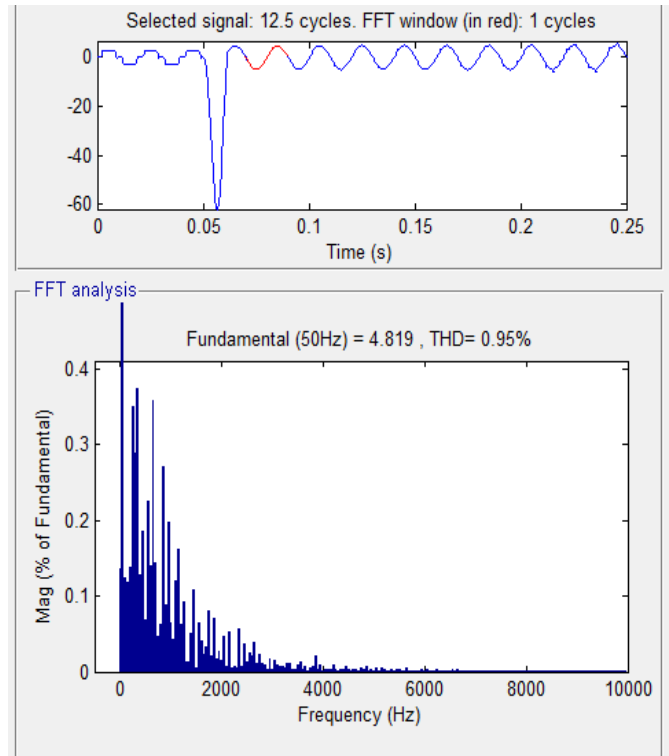


Fig. 15 FFT Analysis of Phase-A Source Current with Fuzzy Controlled APF.

Fig.15 shows the FFT Analysis of Phase-A Source Current with Fuzzy Controlled APF, here we get 2.52%.

V. CONCLUSION

This proposed model is implemented using Matlab Simulink software and the obtained resultant waveforms were evaluated and the effectiveness of the system stability and performance of power system have been established. Improved dynamic current harmonics and a reactive power compensation scheme for power distribution systems with generation from renewable sources has been proposed to improve the current quality of the distribution system. Advantages of the proposed scheme are related to its simplicity, modeling, and implementation. This paper has presented a novel control of an existing RES interfacing APF using conventional PI controller & fuzzy logic controller to improve the quality of power at PCC for a 3-phase 4-wire system. It has been shown that the APF system can be effectively utilized for power conditioning without affecting its normal operation of real power transfer. By using conventional controller we get THD value is 2.52%, but using the fuzzy logic controller THD value is 0.95%.

VI. REFERENCES

- [1] J. Rocabert, A. Luna, F. Blaabjerg, and P. Rodriguez, —Control of power converters in AC microgrids,|| IEEE Trans. Power Electron., vol. 27, no. 11, pp. 4734–4749, Nov. 2012.
- [2] M. Aredes, J. Hafner, and K. Heumann, —Three-phase four-wire shunt active filter control strategies,|| IEEE Trans. Power Electron., vol. 12, no. 2, pp. 311–318, Mar. 1997.
- [3] S. Naidu and D. Fernandes, —Dynamic voltage restorer based on a fourleg voltage source converter,|| Gener. Transm. Distrib., IET, vol. 3, no. 5, pp. 437–447, May 2009.

- [4] N. Prabhakar and M. Mishra, —Dynamic hysteresis current control to minimize switching for three-phase four-leg VSI topology to compensate nonlinear load,|| IEEE Trans. Power Electron., vol. 25, no. 8, pp. 1935–1942, Aug. 2010.
- [5] G.Satyanarayana., K.N.V Prasad, G.Ranjith Kumar, K. Lakshmi Ganesh, "Improvement of power quality by using hybrid fuzzy controlled based IPQC at various load conditions," Energy Efficient Technologies for Sustainability (ICEETS), 2013 International Conference on , vol., no., pp.1243,1250, 10-12 April 2013..
- [6] F. Wang, J. Duarte, and M. Hendrix, —Grid-interfacing converter systems with enhanced voltage quality for microgrid application;concept and implementation,|| IEEE Trans. Power Electron., vol. 26, no. 12, pp. 3501– 3513, Dec. 2011.
- [7] X.Wei, —Study on digital pi control of current loop in active power filter,|| in Proc. 2010 Int. Conf. Electr. Control Eng., Jun. 2010, pp. 4287–4290.
- [8] R. de Araujo Ribeiro, C. de Azevedo, and R. de Sousa, —A robust adaptive control strategy of active power filters for power-factor correction, harmonic compensation, and balancing of nonlinear loads,|| IEEE Trans. Power Electron., vol. 27, no. 2, pp. 718–730, Feb. 2012.
- [9] J. Rodriguez, J. Pontt, C. Silva, P. Correa, P. Lezana, P. Cortes, and U. Ammann, —Predictive current control of a voltage source inverter,|| IEEE Trans. Ind. Electron., vol. 54, no. 1, pp. 495–503, Feb. 2007.
- [10] Satyanarayana, G.; Ganesh, K.Lakshmi; Kumar, Ch. Narendra; Krishna, M.Vijaya, "A critical evaluation of power quality features using Hybrid Multi-Filter Conditioner topology," Green Computing, Communication and Conservation of Energy (ICGCE), 2013 International Conference on , vol., no., pp.731,736, 12-14 Dec. 2013.
- [11] R. Vargas, P. Cortes, U. Ammann, J. Rodriguez, and J. Pontt, —Predictive control of a three-phase neutral-point-clamped inverter,|| IEEE Trans. Ind. Electron., vol. 54, no. 5, pp. 2697–2705, Oct. 2007.
- [12] P. Cortes, A. Wilson, S. Kouro, J. Rodriguez, and H. Abu-Rub, —Model predictive control of multilevel cascaded H-bridge inverters,|| IEEE Trans. Ind. Electron., vol. 57, no. 8, pp. 2691–2699, Aug. 2010.
- [13] P. Lezana, R. Aguilera, and D. Quevedo, —Model predictive control of an asymmetric flying capacitor converter,|| IEEE Trans. Ind. Electron., vol. 56, no. 6, pp. 1839–1846, Jun. 2009.
- [14] P. Correa, J. Rodriguez, I. Lizama, and D. Andler, —A predictive control scheme for current-source rectifiers,|| IEEE Trans. Ind. Electron., vol. 56, no. 5, pp. 1813–1815, May 2009.
- [15] M. Rivera, J. Rodriguez, B. Wu, J. Espinoza, and C. Rojas, —Current control for an indirect matrix converter with filter resonance mitigation,|| IEEE Trans. Ind. Electron., vol. 59, no. 1, pp. 71–79, Jan. 2012.
- [16] P. Correa, M. Pacas, and J. Rodriguez, —Predictive torque control for inverter-fed induction machines,|| IEEE Trans. Ind. Electron., vol. 54, no. 2, pp. 1073–1079, Apr. 2007.
- [17] M. Odavic, V. Biagini, P. Zanchetta, M. Sumner, and M. Degano, —Onesample- period-ahead predictive current control for high-performance active shunt power filters,|| Power Electronics, IET, vol. 4, no. 4, pp. 414–423, Apr. 2011.
- [18] IEEE Recommended Practice for Electric Power Distribution for Industrial Plants, IEEE Standard 141-1993, 1994.
- [19] R. de Araujo Ribeiro, C. de Azevedo, and R. de Sousa, —A robust adaptive control strategy of active power filters for power-factor correction, harmonic compensation, and balancing of nonlinear loads,|| IEEE Trans. Power Electron., vol. 27, no. 2, pp. 718–730, Feb. 2012.
- [20] M. Sumner, B. Palethorpe, D. Thomas, P. Zanchetta, and M. Di Piazza, —A technique for power supply harmonic impedance estimation using a controlled voltage disturbance,|| IEEE Trans. Power Electron., vol. 17, no. 2, pp. 207–215, Mar. 2002.
- [21] S. Ali, M. Kazmierkowski, —PWM voltage and current control of four-leg VSI,|| presented at the ISIE, Pretoria, South Africa, vol. 1, pp. 196–201, Jul. 1998.
- [22] S. Kouro, P. Cortes, R. Vargas, U. Ammann, and J. Rodriguez, —Model predictive control—A simple and powerful method to control power converters,|| IEEE Trans. Ind. Electron., vol. 56, no. 6, pp. 1826–1838, Jun. 2009.